

# We are IntechOpen, the world's leading publisher of Open Access books Built by scientists, for scientists

6,900

Open access books available

185,000

International authors and editors

200M

Downloads

Our authors are among the

154

Countries delivered to

TOP 1%

most cited scientists

12.2%

Contributors from top 500 universities



WEB OF SCIENCE™

Selection of our books indexed in the Book Citation Index  
in Web of Science™ Core Collection (BKCI)

Interested in publishing with us?  
Contact [book.department@intechopen.com](mailto:book.department@intechopen.com)

Numbers displayed above are based on latest data collected.  
For more information visit [www.intechopen.com](http://www.intechopen.com)



# Inverse Measurement of the Thickness and Flow Resistivity of Porous Materials via Reflected Low Frequency Waves-Frequency Approach

*Mustapha Sadouki*

## Abstract

A direct and inverse method is proposed for measuring the thickness and flow resistivity of a rigid air-saturated porous material using acoustic reflected waves at low frequency. The equivalent fluid model is considered. The interactions between the structure and the fluid are taken by the dynamic tortuosity of the medium introduced by Johnson et al. and the dynamic compressibility of the air introduced by Allard. A simplified expression of the reflection coefficient is obtained at very low frequencies domain (Darcy's regime). This expression depends only on the thickness and flow resistivity of the porous medium. The simulated reflected signal of the direct problem is obtained by the product of the experimental incident signal and the theoretical reflection coefficient. The inverse problem is solved numerically by minimizing between simulated and experimental reflected signals. The tests are carried out using two samples of polyurethane plastic foam with different thicknesses and resistivity. The inverted values of thickness and flow resistivity are compared with those obtained by conventional methods giving good results.

**Keywords:** acoustic characterization, porous materials, fluid equivalent model, reflected wave, Darcy's regime

## 1. Introduction

Porous materials are of great importance for a wide range of industrial and engineering applications, including transportation, construction, aerospace, bio-medical and others. These materials, such as plastic foams, fibers and granular materials are frequently used for sound and heat insulation in buildings, schools and hospitals to minimize noise and reduce nuisance.

The propagation of sound in a porous material is a phenomenon that governed by physical characteristics of a porous medium. Porous sound absorbers are materials in which sound propagation takes place in a network of interconnected pores such that the viscous and thermal interaction causes the dissipation of acoustic energy and converts it into heat. Knowledge of the acoustic and physical properties of these materials is of great importance in predicting their acoustic behavior and

their insulate ability against noise and heat. For this reason, there are many works of research and studies in the literature [1–15] that are articulated in this line of inquiry where many mathematical and semi-phenomenological models have been developed to study the acoustic behavior of these materials. Among the most important of these models, we find the JCA model (Johnson-Champoux-Allard model) [1–4] used in the case of porous materials with a rigid structure saturated with air.

According to the JCA model [3, 4], The acoustic propagation in air saturated porous materials is described by the inertial, viscous, and thermal interactions between the fluid and the structure [1–5]. In the high frequency domain [1–4] the inertial, viscous and thermal interactions are taken into account, by the high limit of tortuosity for the inertial effects [3], and by the viscous and thermal characteristic length [1, 2, 4] for the viscous and thermal effects. In the low-frequency domain [1, 2, 11, 13], inertial, viscous and thermal interactions are described by the inertial and thermal tortuosity and by the viscous and thermal permeability. In very low frequency approximation, the viscous-inertial interactions [11, 14, 15] are only described by the flow resistivity. The determination of these parameters is crucial for the prediction of sound damping in these materials.

The objective of this work is to propose an acoustic method based on the resolution of the direct and inverse problem using reflected acoustic waves at low frequency to determine the thickness and flow resistivity describing the porous medium. The direct problem consists in constructing theoretically the reflected signal knowing the incident signal and the parameters of the medium; given the experimental incident signal denoted by  $p_{exp}^i(\omega)$ , and the reflection coefficient which plays the role of a transfer function of the medium denoted  $R(\sigma, L, \omega)$  as a function of the parameters to be found, we deduce the simulated reflected signal  $p_{sim}^r(\sigma, L, \omega)$  which must be compared to the experimental reflected signal  $p_{exp}^r(\omega)$ . The inverse problem therefore consists in minimizing the difference between the  $p_{exp}^r(\omega)$  and  $p_{sim}^r(\sigma, L, \omega)$  signals by varying the required parameters. The solution corresponds to the sets of parameters that give the minimum deviation between the simulated reflected signal and the experimental reflected signal.

## 2. Acoustical model

The porous material is a bi-phasic medium consisting of a solid part and a fluid part that saturates the pores. When the solid part is flexible, the two phases start moving simultaneously under excitation by an acoustic wave; in this case the dynamics of the movement is well described by Biot's theory [16–18]. In the case of a rigid material, the solid part remains immobile and the acoustic waves propagate only in the fluid. This case is described by the equivalent fluid theory [1–5]. In this theory the viscous and inertial interactions within the medium are described by the dynamic tortuosity introduced by Johnson et al. [2, 3] while the thermal effects are taken into account by the dynamic compressibility of the fluid given by Allard and Champoux [1, 4]. In the frequency domain, these factors are multiplied by the density and compressibility of the fluid.

To differentiate between high and low frequency regimes [1–3], the viscous and thermal layer thicknesses  $\delta = \sqrt{2\eta/\omega\rho}$  and  $\delta' = \delta/\sqrt{Pr}$  are compared, at a given frequency, with the effective radius of the pores  $r$  ( $\rho$  is the density of the saturation fluid,  $\omega$  the pulsation frequency,  $Pr$  the Prandtl number, and  $\eta$  the viscosity of the fluid). The low frequency range is defined when the viscous [3] and thermal [1] skin thicknesses are great relatively to the pore radius. Otherwise, it is the high-frequency range. In the Darcy regime (flow without inertial effect), corresponding

to the very low frequencies [11, 15], the air flow resistivity is the most important parameter describing the viscous losses caused by fluid/structure exchanges. In this case, the dynamic tortuosity  $\alpha(\omega)$  and the dynamic compressibility  $\beta(\omega)$  are given by [2, 3, 13–15, 19]:

$$\alpha(\omega) = \frac{\sigma\phi}{j\omega\rho} \tag{1}$$

$$\beta(\omega) = \gamma \tag{2}$$

In these equations,  $j^2 = -1$ ,  $\phi$  is the porosity,  $\sigma$  is the flow resistivity,  $\rho$  is saturating fluid density and  $\gamma$  is the adiabatic constant.

Let us consider an acoustic wave arriving under normal incidence and striking a homogeneous porous material that occupies the region  $0 \leq x \leq L$  (**Figure 1**). This wave generates an acoustic pressure field  $p$  and an acoustic velocity field  $v$  within the material that satisfies the following macroscopic equivalent fluid equations (along the x-axis):

$$\rho\alpha(\omega)j\omega v = \frac{\partial p}{\partial x}, \quad \frac{\beta(\omega)}{K_a}j\omega p = \frac{\partial v}{\partial x} \tag{3}$$

where  $K_a$  is the compressibility modulus of the fluid.

The expression of a pressure field incident plane, unit amplitude, arriving at normal incidence to the porous material is given by

$$p^i(x, \omega) = e^{-j(kx - \omega t)}, \tag{4}$$

where  $k = \frac{\omega}{c_0} = \omega\sqrt{\frac{\rho_0}{K_a}}$ ,  $k$  and  $c_0$  are, respectively, the wave number and the wave velocity of the free fluid.

In the medium (1) ( $x < 0$ ), the movement's results from the superposition of incident and reflected waves,

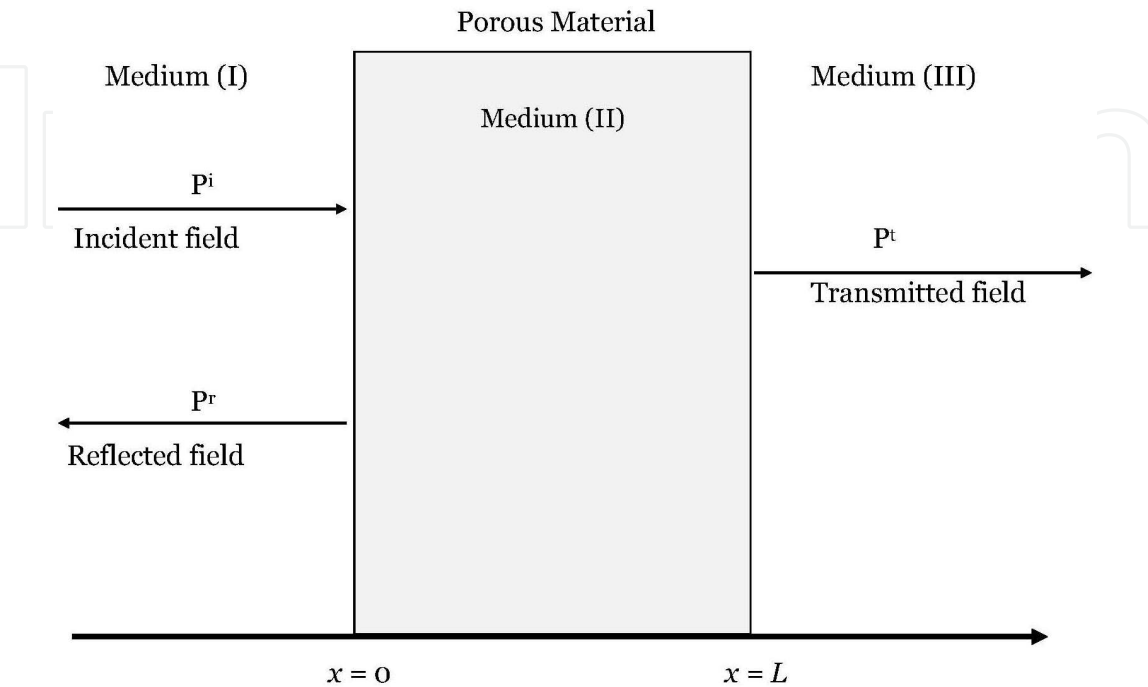


**Figure 1.**  
Problem geometry.

$$p_1(x, \omega) = e^{-j(kx - \omega t)} + \tilde{R}e^{-j(-kx - \omega t)} \quad (5)$$

where  $\tilde{R}$  is the reflection coefficient.

According to Eq. (3), the expression of the velocity field in the medium (1) is written:

$$v_1(x, \omega) = \frac{1}{Z_0} \left( e^{-j(kx - \omega t)} - \tilde{R}e^{-j(-kx - \omega t)} \right) \quad (6)$$

where  $Z_0 = \sqrt{\rho_0 K_a}$  is the characteristic impedance of air.

In the medium (2) corresponding to the porous material, the expressions of the pressure and velocity field are:

$$p_2(x, \omega) = \tilde{A}e^{-j(\tilde{k}x - \omega t)} + \tilde{B}e^{-j(-\tilde{k}x - \omega t)} \quad (7)$$

$$v_2(x, \omega) = \frac{1}{\tilde{Z}_c} \left( \tilde{A}e^{-j(\tilde{k}x - \omega t)} - \tilde{B}e^{-j(-\tilde{k}x - \omega t)} \right) \quad (8)$$

In these expressions  $\tilde{A}$  and  $\tilde{B}$  are amplitude constants of the right-going and left-going waves,  $\tilde{Z}_c$  and  $\tilde{k}$  are the characteristic impedance and wave number, respectively, of the acoustic wave in the porous medium. These are two complex quantities:

$$\tilde{k} = \omega \sqrt{\frac{\tilde{\rho}}{\tilde{K}}} = \omega \sqrt{\frac{\rho_0 \alpha(\omega) \beta(\omega)}{K_a}}, \text{ and } \tilde{Z}_c = \sqrt{\tilde{\rho} \tilde{K}} = \sqrt{\frac{\rho_0 K_a \alpha(\omega)}{\beta(\omega)}} \quad (9)$$

Finally, in the medium (3), the expressions of the pressure and velocity fields of the wave transmitted through the porous material are,

$$p_3(x, \omega) = \tilde{T}e^{-j(k(x-L) - \omega t)}, \quad (10)$$

$$v_3(x, \omega) = \frac{1}{Z_0} \tilde{T}e^{-j(k(x-L) - \omega t)} \quad (11)$$

In these Eqs. ((10) and (11))  $\tilde{T}$  is the transmission coefficient.

The continuity conditions of the pressure field and of the velocity field at the boundary of the medium are given by:

$$p_1(0^-, \omega) = p_2(0^+, \omega) \quad p_2(L^-, \omega) = p_3(L^+, \omega) \quad (12)$$

$$v_1(0^-, \omega) = \phi v_2(0^+, \omega) \quad \phi v_2(L^-, \omega) = v_3(L^+, \omega) \quad (13)$$

the  $\pm$  superscript denotes the limit from right and left, respectively. Using boundary and initial condition (12)–(13), reflected coefficient can be derived:

$$\tilde{R}(\omega) = \frac{(\phi^2 - \tilde{Z}^2) \sinh(j\tilde{k}L)}{2\phi\tilde{Z} \cosh(j\tilde{k}L) + (\phi^2 + \tilde{Z}^2) \sinh(j\tilde{k}L)} \quad (14)$$

where  $\tilde{Z} = \frac{\tilde{Z}_c}{Z_0} = \sqrt{\frac{\alpha(\omega)}{\beta(\omega)}}$  is the normalized characteristic impedance of the material.

Using the expressions of the dynamic tortuosity  $\alpha(\omega)$  and the dynamic compressibility  $\beta(\omega)$  given by Eq.(1), the expression (14) of the reflection coefficient becomes:

$$R(\omega) = \frac{(1 - C_1^2 \omega) \sinh(LC_2 \sqrt{j\omega})}{2C_1 \sqrt{j\omega} \cosh(LC_2 \sqrt{j\omega}) + (1 + C_1^2 \omega) \sinh(LC_2 \sqrt{j\omega})} \quad (15)$$

where

$$C_1 = \sqrt{\frac{\gamma \rho \phi}{\sigma}} \text{ et } C_2 = \sqrt{\frac{\gamma \sigma \phi}{K_a}} \quad (16)$$

By doing the Taylor series expansion of the reflection coefficient (Eq. (15)), limited to the first approximation, the reflection coefficient expression is written at very low frequencies (see appendix):

$$R = \frac{1}{1 + \frac{2}{L\sigma} \sqrt{\rho K_a}} \quad (17)$$

This simplified expression of the reflection coefficient is independent of the frequency and porosity of the material, and depends only on the flow resistivity  $\sigma$  and the thickness  $L$  of the material.

The incident  $p^i$  and reflected  $p^r$  fields are related in the frequency domain by the reflection coefficient  $R$ :

$$p_{sim}^r(x, \omega) = R p^i(x, \omega) \quad (18)$$

The time-domain simulated reflected signals  $\mathcal{P}_{sim}^r(x, t)$  are obtained numerically by taking the inverse Fourier transform  $\mathcal{F}^{-1}$  of (18),

$$\mathcal{P}_{sim}^r(x, t) = \mathcal{F}^{-1}(R p^i(x, \omega)) \quad (19)$$

### 3. Inverse problem

The simplified expression of the reflection coefficient obtained at low frequency (Eq.(17)) depends only on the flow resistivity  $\sigma$  and thickness  $L$  of the medium. Our objective is to find this two parameters simultaneously, supposedly unknown, by minimizing between the simulated reflected signal given by the expression (18) and the experimental reflected signal. The inverse problem then consists in finding the flow resistivity  $\sigma$  and thickness  $L$  of porous samples that minimize the function:

$$U(\sigma, L) = \sum_{i=1}^{i=N} \left( p_{exp}^r(\omega) - p_{sim}^r(\sigma_i, L_i, \omega) \right)^2 \quad (20)$$

Wherein  $p_{sim}^r(\sigma_i, L_i, \omega)$  are the discrete sets values of the simulated reflected signal and  $p_{exp}^r(x, \omega)$  are the discrete sets of values of the experimental reflected signal. The minimization is made in frequency domain. The experimental setup [15] is shown in **Figure 2**. The tube length is adaptable to avoid reflection, and to permit the propagation of transient signals, according to the desired frequency range. For measurements in the frequency range (20–100) Hz, a length of 50 m is sufficient. The tube diameter is 5 cm (the cut-off of the tube  $f_c \sim 4$  kHz). A sound source Driver unit “Brand” constituted by loudspeaker Realistic 40–9000 is used. Tone-bursts are provided by Standard Research Systems Model DS345–30 MHz synthesized function generator. The signals are amplified and filtered using model



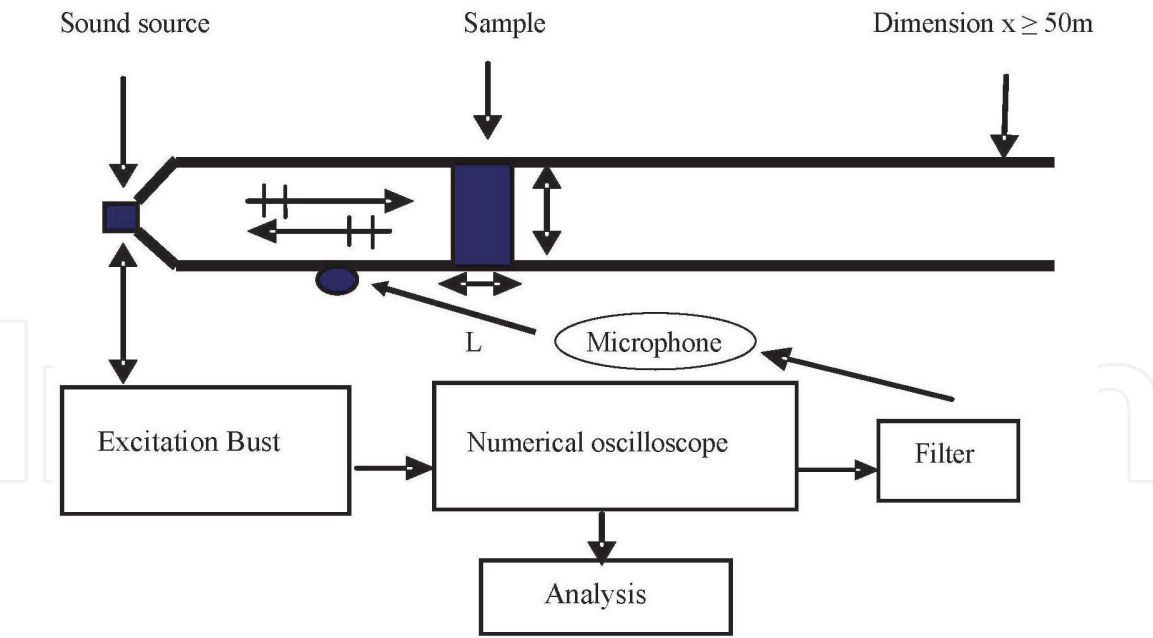


**Figure 2.**  
*The experimental set up.*

SR 650-Dual channel filter, Stanford Research Systems. The signals (incident and reflected) are measured using the same microphone. The incident signal is measured by putting a total reflector [15] in the same position as the porous sample. **Figures 3, 4** show the incident and reflected signals and their spectrum of the two samples in frequency bandwidth of 50 Hz.

The inverse problem is solved for two cylindrical polyurethane (PU) foams named (M1) and (M2) with a rigid frame and an open cell structure. Polyurethane foam is a leading member of the large and very diverse family of polymers or plastics and has many uses in the automotive sector and for the thermal insulation of buildings. The flow resistivity and thicknesses of the two samples M1 and M2 are measured by conventional methods [20, 21] and given in **Table 1**.

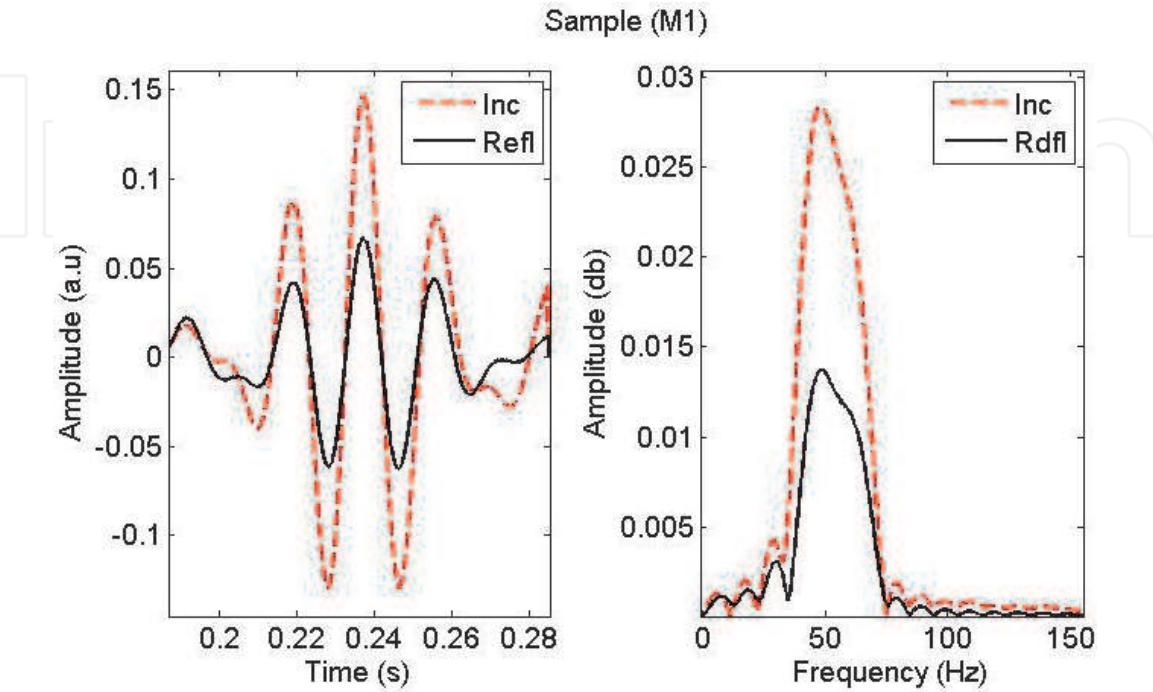


**Figure 3.**  
*The incident and reflected signals and their spectrum of the sample (M1) in frequency bandwidth of 50 Hz.*

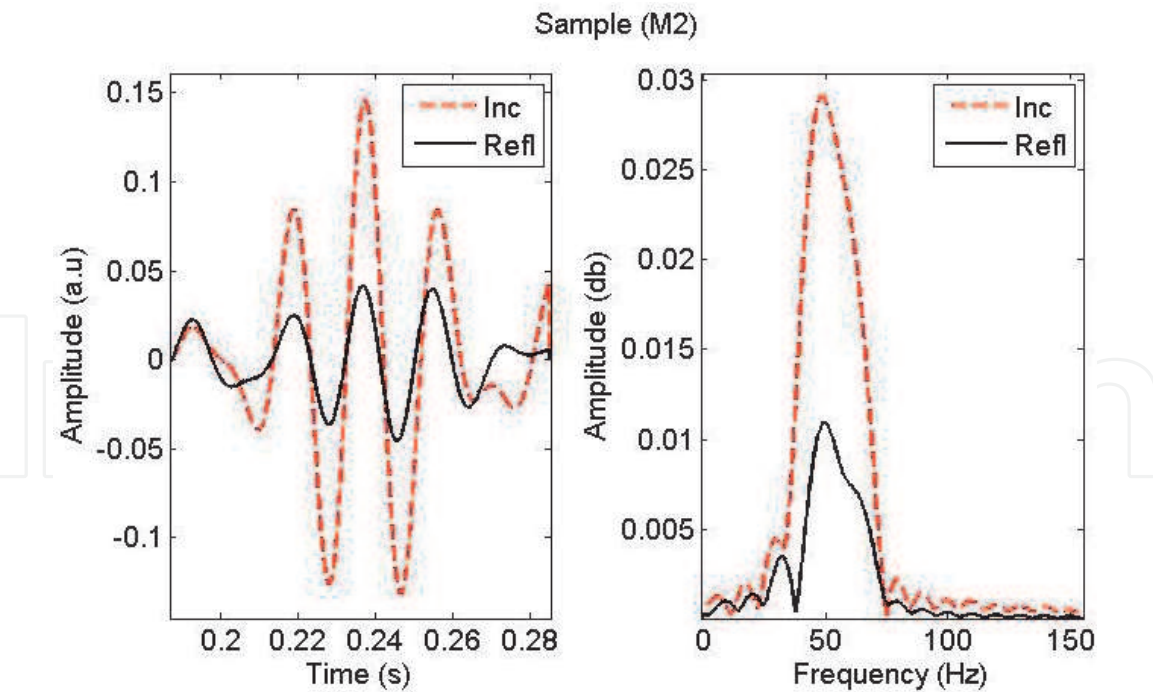


**Figure 4.**  
The incident and reflected signals and their spectrum of the sample (M2) in frequency bandwidth of 50 Hz.

Samples	M1	M2
Thickness (cm)	2.6 ± 0.5	5.0 ± 0.5
Resistivity (Nm <sup>-4</sup> s)	27,500 ± 500	7500 ± 500

**Table 1.**  
Flow resistivity and thickness of the sample M1 and M2.

The inverse problem is to find the parametric vector  $V = \{\sigma, L\}$  which satisfies the conditions:

$$\begin{cases} U(\sigma, L) \rightarrow 0 \\ LV \leq V \leq UV \end{cases} \quad (21)$$

where  $LV$  and  $UV$  are the lower and upper bounds that limit the research domain on the adjustable parametric vector  $V$ . For plastic foam samples, the value of the flow resistivity is greater than  $3000 \text{ Nm}^{-4}\text{s}$ . The lower and upper limits in Eq. (20) can be built from the following constraints:

$$\begin{cases} \sigma \geq 3000 \text{ Nm}^{-4}\text{s} \\ 0 \leq L \leq 10 \text{ cm} \end{cases} \quad (22)$$

The inverse problem is solved by the last-square method. For its iterative solution, we used the simplex search method [22–26] which does not require numerical or analytic gradient. The flow resistivity and the thickness are inverted using experimental reflected signals by two PU porous material samples (M1 and M2). The variations in the cost function present one clear minimum corresponding to the solution of the inverse problem. **Figures 5, 6** show the variation of the cost function  $U$  when varying the flow resistivity and the thickness in different frequency bandwidths for the samples (M1, M2). The results of the inverse problem



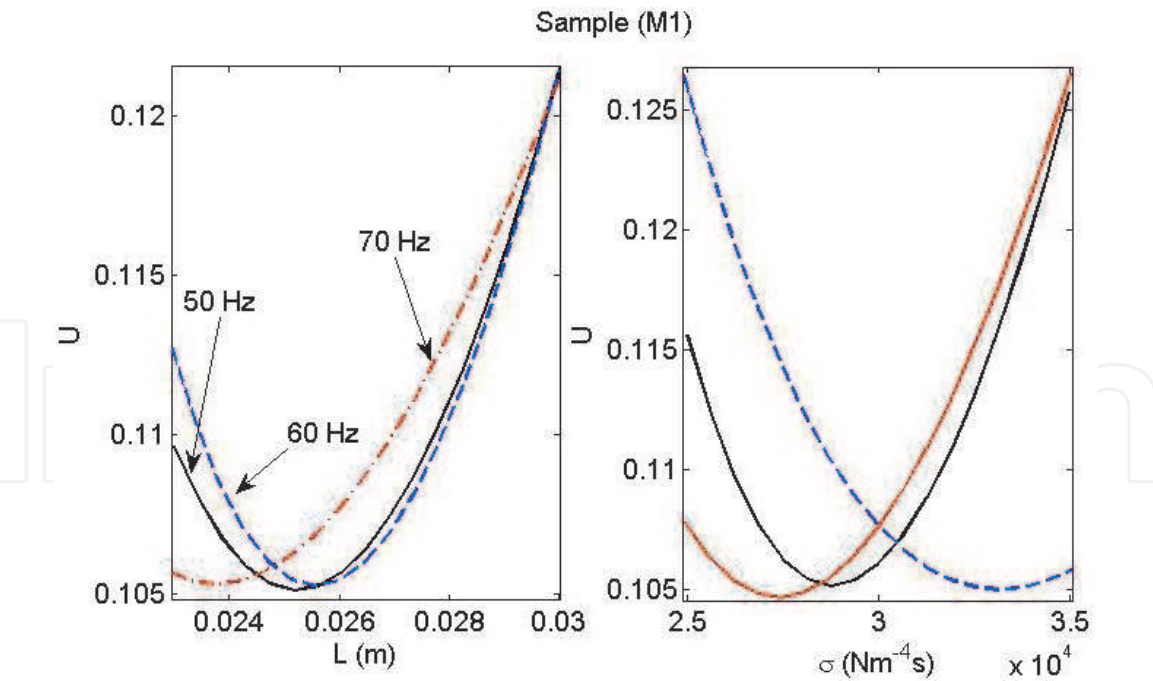


**Figure 5.** Variation of the cost function  $U$  when varying the flow resistivity and the thickness in different frequency bandwidths for the samples M1.

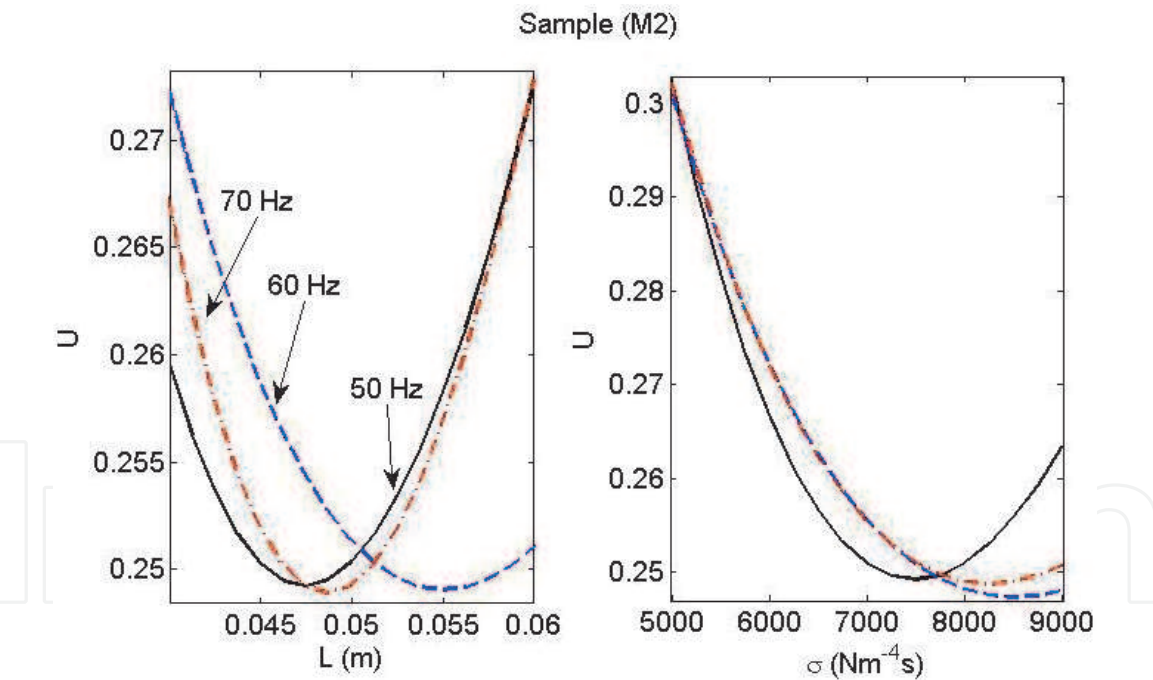


**Figure 6.** Variation of the cost function  $U$  when varying the flow resistivity and the thickness in different frequency bandwidths for the samples M2.

are summarized in **Table 2**, in which inverted values of flow resistivity and thickness are given for different frequency bandwidths. A comparison between an experimental reflected signal and simulated reflected signal is given in **Figures 7, 8** for the optimized values of the inverted flow resistivity and thickness of the porous samples (M1, M2), respectively. The frequency bandwidth of the incident signals is (40–60) Hz. It can be seen that the agreement between experiment and theory is good for the two samples and the inverted values are close to those given by conventional methods.

Samples	Frequency (Hz)	Thickness (cm)	Resistivity (Nm <sup>-4</sup> s)
M1	50	2.52	28,750
	60	2.56	33,125
	70	2.39	27,500
M2	50	4.75	7500
	60	5.55	8500
	70	4.88	8250

**Table 2.**  
*Inverted parameters obtained of the flow resistivity and the thickness of the two samples M1 and M2.*

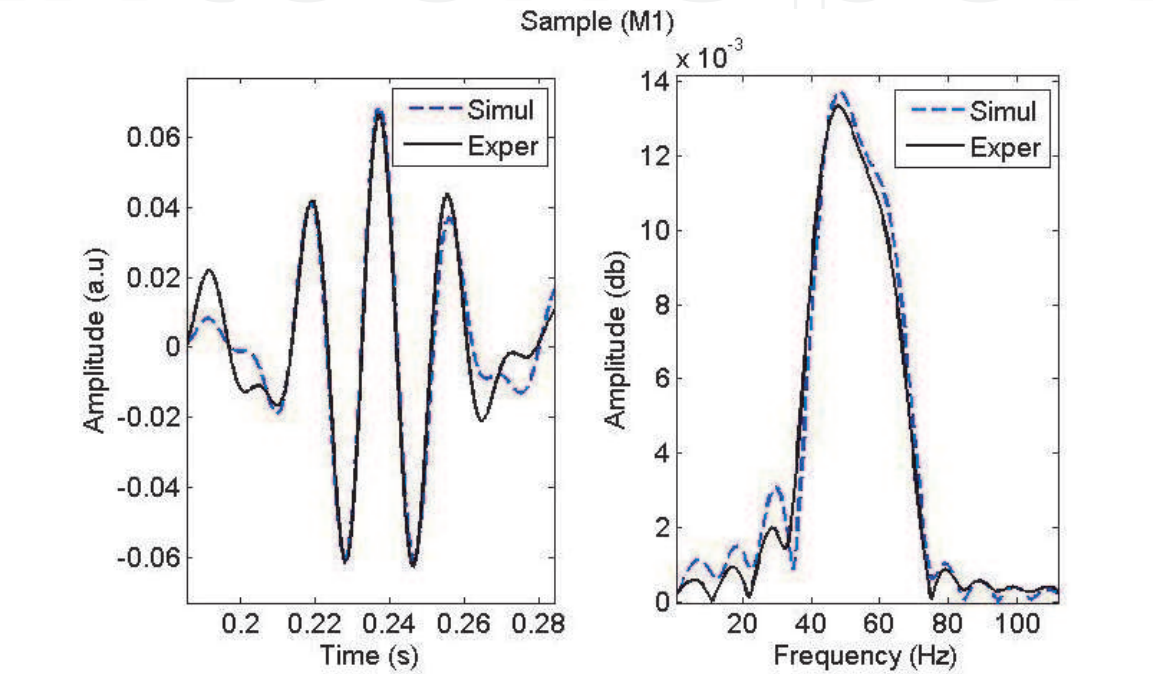


**Figure 7.**  
*Comparison between an experimental reflected signal and simulated reflected signal of the sample M1.*

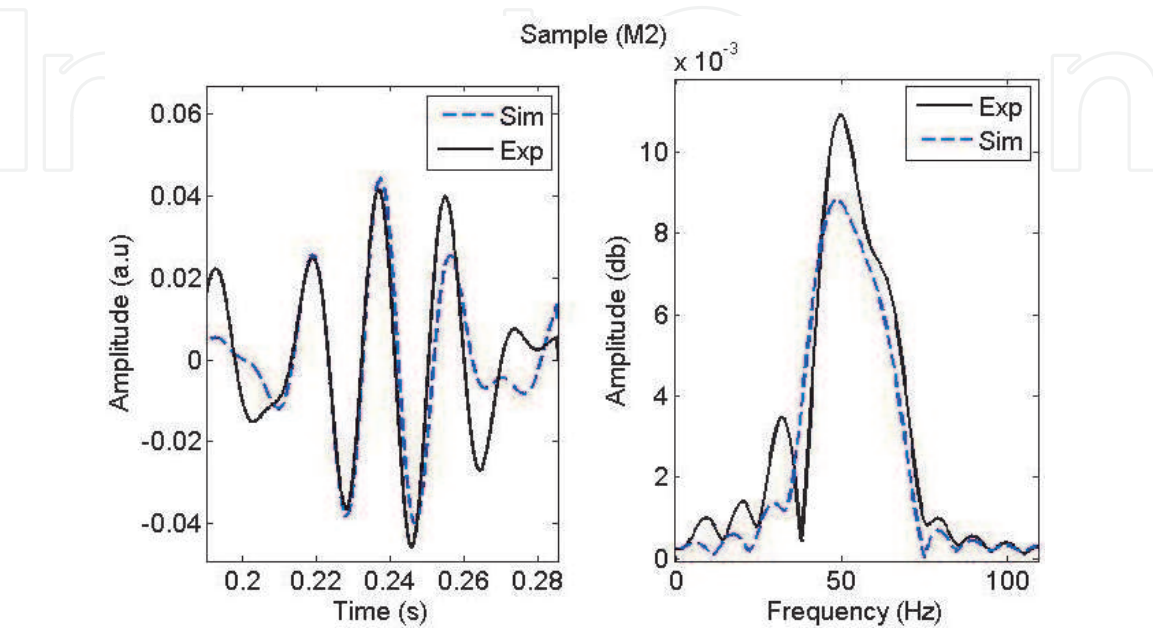


**Figure 8.**  
*Comparison between an experimental reflected signal and simulated reflected signal of the sample M2.*

## 4. Conclusion

Simultaneous determination of the flow resistivity and the thickness of a rigid porous medium are obtained by solving the inverse problem using experimental signals at very low frequencies. The model is based on a simplified expression of the reflection coefficient which is independent on frequency and porosity and depends only on the flow resistivity and thickness of the medium. Two plastic foam samples having different values of flow resistivity and different thickness are tested using this proposed method. The results are satisfactory and the inverted values of flow resistivity and thickness are close to those given by conventional methods. The advantage of the proposed method is that the two parameters, resistivity and thickness of the porous medium, were determined simultaneously without knowing previously any other parameter describing the porous medium, including its porosity. The suggested method opens new perspectives for the acoustic characterization of porous materials.

## Acknowledgements

This work is funded by the university training research project (PRFU) under number: B00L02UN440120200001 and by the General Direction of Scientific Research and Technological Development (DGRSDT).

## Conflict of interest

The authors declare that they have no conflict of interest.

## Appendix: Taylor series expansion of the reflection coefficient

The reflection coefficient given by Eq. (15) can be rewritten as [14, 15]:

$$R(\omega) = \left( \frac{1 - C_1^2 j\omega}{1 + C_1^2 j\omega} \right) \left( \frac{1}{1 + \coth(LC_2 \sqrt{j\omega}) \frac{2C_1 \sqrt{j\omega}}{1 + C_1^2 j\omega}} \right) \quad (\text{A.1})$$

where  $C_1$  and  $c_2$  are given by Eq. (16). Taylor's limited serial expansion in the vicinity of zero of the expressions  $\left( \frac{1 - C_1^2 j\omega}{1 + C_1^2 j\omega} \right)$ ,  $\frac{2C_1 \sqrt{j\omega}}{1 + C_1^2 j\omega}$  and  $\coth(LC_2 \sqrt{j\omega})$  is given by:

$$\left( \frac{1 - C_1^2 j\omega}{1 + C_1^2 j\omega} \right) = 1 - 2C_1^2 j\omega + \mathcal{O}\left((j\omega)^2\right), \quad (\text{A.2})$$

$$\frac{2C_1 \sqrt{j\omega}}{1 + C_1^2 j\omega} = 2C_1 \sqrt{j\omega} - 2C_1^3 (j\omega)^{3/2} + \mathcal{O}\left((j\omega)^{5/2}\right), \quad (\text{A.3})$$

and,

$$\coth(LC_2 \sqrt{j\omega}) = \frac{1}{LC_2 \sqrt{j\omega}} + \frac{1}{3} LC_2 j\omega - \frac{1}{45} L^3 C_2^3 (j\omega)^{3/2} + \mathcal{O}\left((j\omega)^{5/2}\right), \quad (\text{A.4})$$

with,

$$\coth\left(LC_2\sqrt{j\omega}\right)\frac{2C_1\sqrt{j\omega}}{1+C_1^2j\omega}=\frac{2C_1}{LC_2}+\frac{2}{3}C_1C_2L\left(1-\frac{3C_1^2}{L^2C_2^2}\right)j\omega+\mathcal{O}\left((j\omega)^2\right), \quad (\text{A.5})$$

and,

$$\frac{1}{1+\coth\left(LC_2\sqrt{j\omega}\right)\frac{2C_1\sqrt{j\omega}}{1+C_1^2j\omega}}=\frac{1}{1+\frac{2C_1}{LC_2}}-\frac{\frac{2}{3}L^3C_2^3C_1\left(1-\frac{3C_1^2}{L^2C_2^2}\right)}{\left(1+\frac{2C_1}{LC_2}\right)^2}j\omega+\mathcal{O}\left((j\omega)^2\right), \quad (\text{A.6})$$

Using Eqs. (A.1), (A.2) and (A.6), one obtains

$$R(\omega)=\left(\frac{1}{1+\frac{2C_1}{LC_2}}\right)\left(1-\frac{\frac{2}{3}LC_1C_2\left(1+\frac{3C_1}{LC_2}+3\frac{3C_1^2}{L^2C_2^2}\right)}{\left(1+\frac{2C_1}{LC_2}\right)}j\omega+\mathcal{O}\left((j\omega)^2\right)\right) \quad (\text{A.7})$$

As a first approximation, at very low frequencies, the reflection coefficient (A.7) is given by the first term

$$R=\frac{1}{1+\frac{2C_1}{LC_2}}=\frac{1}{1+\frac{2}{L\sigma}\sqrt{\rho K_a}} \quad (\text{A.8})$$


## Author details

Mustapha Sadouki

Acoustics and Civil Engineering Laboratory, Matter Sciences Department, Faculty of Sciences and Technology, Khemis-Miliana University, BP. 44225 Ain Defla, Algeria

\*Address all correspondence to: [mustapha.sadouki@univ-dbkm.dz](mailto:mustapha.sadouki@univ-dbkm.dz)

## IntechOpen

© 2020 The Author(s). Licensee IntechOpen. This chapter is distributed under the terms of the Creative Commons Attribution License (<http://creativecommons.org/licenses/by/3.0>), which permits unrestricted use, distribution, and reproduction in any medium, provided the original work is properly cited. 

## References

- [1] Allard. J. F, Propagation of Sound in Porous Media Modelling. Sound Absorbing Materials. Elsevier, London, UK, 1993, p. 1–284; DOI 10.1007/978-94-011-1866-8
- [2] Lafarge D, Materials and Acoustics Handbook, edited by M. Bruneau and C. Potel. ISTE-Wiley, London, 2009, p. 149–202.
- [3] Johnson D. L, Koplik J, and Dashen R, “Theory of dynamic permeability and tortuosity in fluid-saturated porous media,” *J. Fluids Mech.* 1987; 176–379; <https://doi.org/10.1017/S0022112087000727>
- [4] Champoux Y, and Allard J. F, Dynamic tortuosity and bulk modulus in air-saturated porous media. *J. Appl. Phys.* 1991; 70: 1975–1979; <https://doi.org/10.1063/1.349482>
- [5] Zwikker C, and Kosten C. W, Sound Absorbing Materials. Elsevier, 1949, New York.
- [6] Henry M, Lemarinier P, Allard J. F, Bonardet J. L, and Gedeon A, Evaluation of the characteristic dimension for porous sound absorbing materials. *J. Appl. Phys.* 1995;77: 17–20.
- [7] Tizianel J, Allard J. F, Castagnède B, Ayrault C, Henry M and Moussatov A, Transport parameters and sound propagation in an air-saturated sand. *J. Appl. Phys. Am.* 1999; 86: 5829; <https://doi.org/10.1063/1.371599>
- [8] Attenborough K, On the acoustic slow wave in air-filled granular media. *J. Acoust. Soc. Am.* 1987; 81, 93; <https://doi.org/10.1121/1.394938>
- [9] Nagy P. B, Adler L, and Bonner B. P, Slow wave propagation in air-filled porous materials and natural rocks. *Appl. Phys. Lett.* 1990;56: 2504; <https://doi.org/10.1063/1.102872>
- [10] Delaney M, and Bazley E, Acoustical properties of fibrous absorbent materials, *Appl. Acoust.* 1970;3: 105–116; [https://doi.org/10.1016/0003-682X\(70\)90031-9](https://doi.org/10.1016/0003-682X(70)90031-9)
- [11] Sadouki M, Fellah Z. E. A, Berbiche A, Fellah M, Mitri F. G, Ogam E, and Depollier C, Measuring static viscous permeability of porous absorbing materials, *J. Acoust. Soc. Am.* 2014; 135: 3163; <https://doi.org/10.1121/1.4874600>
- [12] Sadouki M, Experimental characterization of rigid porous material via the first ultrasonic reflected waves at oblique incidence. *J. ApAcoust.* 2018;133: 64–72; <https://doi.org/10.1016/j.apacoust.2017.12.010>
- [13] Sadouki M, Experimental Measurement of the porosity and the viscous tortuosity of rigid porous material in low frequency. *Journal of Low Frequency Noise Vibration and Active Control*, 2018;37(2): 385–393; <https://doi.org/10.1177/2F1461348418756016>
- [14] Sadouki M, Theoretical modeling of acoustic propagation in an inhomogeneous porous medium. (in French),( Ph. D. Thesis), Université des sciences et de la technologie ‘ Houari Boumediène’, Algiers, Algeria; 2014,
- [15] Berbiche A, Sadouki M, and Fellah Z.E.A, Fellah M, Mitri F.G, Ogam E, Depollier C, Experimental determination of the viscous flow permeability of porous materials by measuring reflected low frequency acoustic waves. *J. Appl. Phys.* 2016; 119: 014906; <https://doi.org/10.1063/1.4939073>
- [16] Biot M. A, The theory of propagation of elastic waves in a fluid-saturated porous solid, low frequency range. *J. Acoust. Soc. Am.* 1956; 28:168; <https://doi.org/10.1121/1.1908241>



- [17] Sadouki M, Fellah M, Fellah Z.E.A, and Ogam E, Depollier C. Ultrasonic propagation of reflected waves in cancellous bone: Application of Biot theory. ESUCB 2015, 6th European Symposium on Ultrasonic Characterization of Bone, 10–12 June 2015; Corfu, (Greece). p.1–4; DOI: 10.1109/ESUCB.2015.7169900
- [18] Sadouki M, Experimental characterization of human cancellous bone via the first ultrasonic reflected wave – Application of Biot’s theory, J. Ap.Acoust, 2020; 107237: 163; <https://doi.org/10.1016/j.apacoust.2020.107237>
- [19] Sadouki M, Direct problem for reflected wave at the first interface of a rigid porous medium in Darcy’s regime. Proc. Mtgs. Acoust. 2015; 25: 045004; <https://doi.org/10.1121/2.0000200>
- [20] Leonard R. W, Simplified flow resistance measurements. J. Acoust. Soc. Am., 1946; 17: 240; <https://doi.org/10.1063/1.2099510>
- [21] Stinson M. R and Daigle G. A, Electronic system for the measurement of flow resistance, J. Acoust. Soc. Am. 1988;83: 2422. <https://doi.org/10.1121/1.396321>
- [22] Lagarias JC, Reeds JA, Wright MH, et al. Convergence properties of the Nelder-Mead Simplex method in low dimensions. SIAM J Optim 1998; 9: 112–147; <https://doi.org/10.1137/S1052623496303470>
- [23] Sadouk M, Thickness measurement of rigid porous material through reflected acoustic waves at Darcy’s regime, Proc. Mtgs. Acoust. 2018;35: 045003; <https://doi.org/10.1121/2.0000973>.
- [24] Sadouki M., Experimental measurement of tortuosity, viscous and thermal characteristic lengths of rigid porous material via ultrasonic transmitted waves, Proc. Mtgs. Acoust. 2018; 35: 045005; <https://doi.org/10.1121/2.0000991>.
- [25] Sadouki M, Berbiche A, Fellah M, Fellah Z E. A and Depollier C. Characterization of rigid porous medium via ultrasonic reflected waves at oblique incidence, Proc. Mtgs. Acoust. 2015; 25: 045005; <https://doi.org/10.1121/2.0000201>
- [26] Sadouki M, Berbiche A, Fellah M, Fellah Z E. A and Depollier C, Measurement of tortuosity and viscous characteristic length of double-layered porous absorbing materials with rigid-frames via transmitted ultrasonic-wave, Proc. Mtgs. Acoust. 2015; 25: 045001; <https://doi.org/10.1121/2.0000184>.